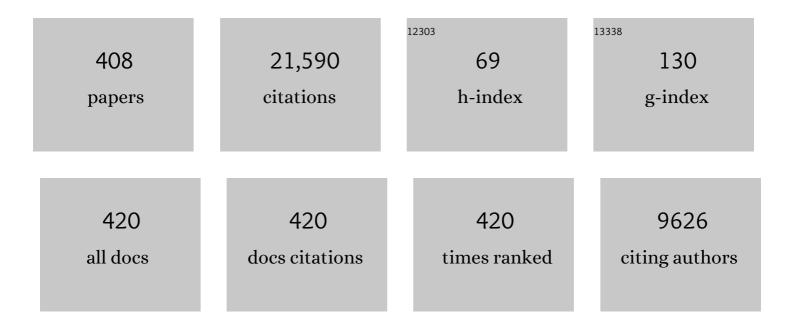
List of Publications by Year in descending order

Source: https://exaly.com/author-pdf/9011379/publications.pdf Version: 2024-02-01



#	Article	IF	CITATIONS
1	Divergent metamorphism within the Namche Barwa Complex, the Eastern Himalaya, Southeast Tibet, China: Insights from in situ U–Th–Pb dating of metamorphic monazite. Journal of Metamorphic Geology, 2022, 40, 307-328.	1.6	5
2	U-Pb speleothem geochronology reveals a major 6 Ma uplift phase along the western margin of Dead Sea Transform. Bulletin of the Geological Society of America, 2022, 134, 1571-1584.	1.6	4
3	Implications for sedimentary transport processes in southwestern Africa: a combined zircon morphology and age study including extensive geochronology databases. International Journal of Earth Sciences, 2022, 111, 767-788.	0.9	4
4	Paleozoic sedimentation and Caledonian terrane architecture in NW Svalbard: indications from U–Pb geochronology and structural analysis. Journal of the Geological Society, 2022, 179, .	0.9	11
5	Timing of magmatic-hydrothermal activity in the Variscan Orogenic Belt: LA-ICP-MS U–Pb geochronology of skarn-related garnet from the Schwarzenberg District, Erzgebirge. Mineralium Deposita, 2022, 57, 1071-1087.	1.7	12
6	Tracing southern Gondwanan sedimentary paths: A case study of northern Namibian late Palaeozoic sedimentary rocks. Sedimentology, 2022, 69, 1738-1768.	1.6	3
7	In situ-produced cosmogenic krypton in zircon and its potential for Earth surface applications. Geochronology, 2022, 4, 65-85.	1.0	1
8	Development of a synorogenic composite sill at deep structural levels of a magmatic arc (Odenwald,) Tj ETQq0 C Structural Geology, 2022, 155, 104525.	0 rgBT /C 1.0	verlock 10 Tf 2
9	Age constraints of the Sturtian glaciation on western Baltica based on U-Pb and Ar-Ar dating of the Lapichi Svita. Precambrian Research, 2022, 371, 106595.	1.2	6
10	Crustal evolution of Western Europe: Constraints from detrital zircon U-Pb-Hf-O isotopes. Gondwana Research, 2022, 106, 379-396.	3.0	5
11	Accessories in Kaiserstuhl carbonatites and related rocks as accurate and faithful recorders of whole rock age and isotopic composition. International Journal of Earth Sciences, 2022, 111, 573-588.	0.9	1
12	Depositional age models in lacustrine systems from zircon and carbonate Uâ€₽b geochronology. Sedimentology, 2022, 69, 2507-2534.	1.6	12
13	New CA-ID-TIMS U–Pb zircon ages for the Altenberg–Teplice Volcanic Complex (ATVC) document discrete and coeval pulses of Variscan magmatic activity in the Eastern Erzgebirge (Eastern Variscan) Tj ETQq1 1	0.084314	rgBT /Overic
14	Spatio-temporal variation of fluid flow behavior along a fold: The Bóixols-Sant Corneli anticline (Southern Pyrenees) from U–Pb dating and structural, petrographic and geochemical constraints. Marine and Petroleum Geology, 2022, 143, 105788.	1.5	16
15	The evolution of the southern Namibian Karoo-aged basins: implications from detrital zircon geochronologic and geochemistry data. International Geology Review, 2021, 63, 1758-1781.	1.1	9
16	100 myr cycles of oceanic lithosphere generation in peri-Gondwana: Neoproterozoic–Devonian ophiolites from the NW African–Iberian margin of Gondwana and the Variscan Orogen. Geological Society Special Publication, 2021, 503, 169-184.	0.8	20
17	Drainage response to Arabia–Eurasia collision: Insights from provenance examination of the Cyprian Kythrea flysch (Eastern Mediterranean Basin). Basin Research, 2021, 33, 26-47.	1.3	6
18	Zircon geochronology and O-Hf isotopes of Cappadocian ignimbrites: New insights into continental crustal architecture underneath the Central Anatolian Volcanic Province, Turkey. Gondwana Research, 2021, 91, 166-187.	3.0	4

#	Article	IF	CITATIONS
19	Early Cambrian oceanic island-arc magmatism at the paleo-Pacific margin of East Gondwana: Evidence from northern Victoria Land (Antarctica). Lithos, 2021, 382-383, 105925.	0.6	1
20	Accurate correction for the matrix interference on laser ablation MC-ICPMS boron isotope measurements in CaCO ₃ and silicate matrices. Journal of Analytical Atomic Spectrometry, 2021, 36, 1607-1617.	1.6	7
21	Precise and accurate Lu–Hf isotope analysis of columbite-group minerals by MC-ICP-MS. Journal of Analytical Atomic Spectrometry, 2021, 36, 1643-1656.	1.6	3
22	Detrital zircon and rutile U–Pb, Hf isotopes and heavy mineral assemblages of Israeli Miocene sands: Fingerprinting the Arabian provenance of the Levant. Basin Research, 2021, 33, 1967-1984.	1.3	2
23	Development of a synorogenic composite sill at deep structural levels of a continental arc (Odenwald, Germany). Part 1: Sederholm-type emplacement portrayed by contact melt in shrinkage cracks. Tectonophysics, 2021, 805, 228774.	0.9	2
24	Compositional variability of Mg/Ca, Sr/Ca, and Na/Ca in the deep-sea bivalve Acesta excavata (Fabricius,) Tj ETQ	0 0 0 rgB	T /Qverlock 10
25	Origin of Graphite–Diamond-Bearing Eclogites from Udachnaya Kimberlite Pipe. Journal of Petrology, 2021, 62, .	1.1	8
26	Reconstructing the metamorphic evolution of the AraçuaÃ-orogen (SE Brazil) using in situ U–Pb garnet dating and <i>P</i> – <i>T</i> modelling. Journal of Metamorphic Geology, 2021, 39, 1145-1171.	1.6	10
27	Metasomatism and deformation of block-in-matrix structures in Syros: The role of inheritance and fluid-rock interactions along the subduction interface. Lithos, 2021, 386-387, 105996.	0.6	17
28	Long-lived intracontinental deformation associated with high geothermal gradients in the Seridó Belt (Borborema Province, Brazil). Precambrian Research, 2021, 358, 106141.	1.2	9
29	Central Asian modulation of Northern Hemisphere moisture transfer over the Late Cenozoic. Communications Earth & Environment, 2021, 2, .	2.6	6
30	Multi-stage sulfur and carbon mobility in fossil continental subduction zones: New insights from carbonate-bearing orogenic peridotites. Geochimica Et Cosmochimica Acta, 2021, 306, 143-170.	1.6	1
31	Two-phase late Paleozoic magmatism (~ 313–312 and ~ 299–298ÂMa) in the Lusatian Block to large scale NW striking fault zones: evidence from zircon U–Pb CA–ID–TIMS geochronology, bulk rock- and zircon chemistry. International Journal of Earth Sciences, 2021, 110, 2923-2953.	and its rel 0.9	ation 7
32	Synâ€rift hydrothermal circulation in the Mesozoic carbonates of the western Adriatic continental palaeomargin (Western Southalpine Domain, NW Italy). Basin Research, 2021, 33, 3045-3076.	1.3	3
33	In-situ U-Pb dating of Ries Crater lacustrine carbonates (Miocene, South-West Germany): Implications for continental carbonate chronostratigraphy. Earth and Planetary Science Letters, 2021, 568, 117011.	1.8	18
34	The Kyrenia Terrane (Northern Cyprus): Detrital Zircon Evidence for Exotic Elements in the Southern Neotethys. Tectonics, 2021, 40, e2021TC006763.	1.3	3
35	U–Pb dating of carbonate veins constraining timing of beef growth and oil generation within Vaca Muerta Formation and compression history in the Neuquén Basin along the Andean fold and thrust belt. Marine and Petroleum Geology, 2021, 132, 105204.	1.5	15
36	U-Pb age of the 2016 Amatrice earthquake causative fault (Mt. Gorzano, Italy) and paleo-fluid circulation during seismic cycles inferred from inter- and co-seismic calcite. Tectonophysics, 2021, 819, 229076.	0.9	10

#	Article	IF	CITATIONS
37	Timing of native metal-arsenide (Ag-Bi-Co-Ni-As±U) veins in continental rift zones – In situ U-Pb geochronology of carbonates from the Erzgebirge/Krušné Hory province. Chemical Geology, 2021, 584, 120476.	1.4	7
38	Formation mechanisms of macroscopic globules in andesitic glasses from the Izu–Bonin–Mariana forearc (IODP Expedition 352). Contributions To Mineralogy and Petrology, 2021, 176, 1.	1.2	4
39	Tracking the Origin and Evolution of Diagenetic Fluids of Upper Jurassic Carbonate Rocks in the Zagros Thrust Fold Belt, NE-Iraq. Water (Switzerland), 2021, 13, 3284.	1.2	7
40	Hydrothermal Fluids and Cold Meteoric Waters along Tectonic-Controlled Open Spaces in Upper Cretaceous Carbonate Rocks, NE-Iraq: Scanning Data from In Situ U-Pb Geochronology and Microthermometry. Water (Switzerland), 2021, 13, 3559.	1.2	9
41	Hydrothermal fluid flow associated to the extensional evolution of the Adriatic rifted margin: Insights from the pre―to postâ€rift sedimentary sequence (SE Switzerland, N ITALY). Basin Research, 2020, 32, 91-115.	1.3	22
42	Phase equilibria constraints on crystallization differentiation: insights into the petrogenesis of the normally zoned Buddusò Pluton in north-central Sardinia. Geological Society Special Publication, 2020, 491, 243-265.	0.8	5
43	U-Pb-Hf isotopic data from detrital zircons in late Carboniferous and Mid-Late Triassic sandstones, and also Carboniferous granites from the Tauride and Anatolide continental units in S Turkey: implications for Tethyan palaeogeography. International Geology Review, 2020, 62, 1159-1186.	1.1	21
44	Testing the preservation potential of early diagenetic dolomites as geochemical archives. Sedimentology, 2020, 67, 849-881.	1.6	45
45	In situ U-Pb dating of hydrothermal diagenesis in tectonically controlled fracturing in the Upper Cretaceous Bekhme Formation, Kurdistan Region-Iraq. International Geology Review, 2020, 62, 2261-2279.	1.1	22
46	Crustal evolution of peri-Gondwana crust into present day Europe: The Serbo-Macedonian and Rhodope massifs as a case study. Lithos, 2020, 356-357, 105295.	0.6	19
47	Disproving the Presence of Paleozoicâ€Triassic Metamorphic Rocks on the Island of Zannone (Central) Tj ETQq1 2020, 39, e2020TC006296.	1 0.7843 1.3	14 rgBT /Ove 15
48	Stacked megafans of the Kalahari Basin as archives of paleogeography, river capture, and Cenozoic paleoclimate of southwestern Africa. Journal of Sedimentary Research, 2020, 90, 980-1010.	0.8	8
49	Evolution of the Kiruna-type Gol-e-Gohar iron ore district, Sanandaj-Sirjan zone, Iran. Ore Geology Reviews, 2020, 127, 103787.	1.1	4
50	U–Pb ages and Hf isotopic compositions of zircon from the Early Miocene Kestanbol Magmatic Complex in NW Anatolia (Turkey): Implications for crustal contribution in the post-collisional magmatism. Journal of Asian Earth Sciences, 2020, 192, 104262.	1.0	1
51	Quantifying deformation processes in the SE Pyrenees using U–Pb dating of fracture-filling calcites. Journal of the Geological Society, 2020, 177, 1186-1196.	0.9	28
52	Structural evolution of continental and marine Permian rock salt of the North German Basin: constraints from microfabrics, geochemistry and U–Pb ages. International Journal of Earth Sciences, 2020, 109, 2369-2387.	0.9	2
53	Exploring laser ablation U–Pb dating of regional metamorphic garnet – The Straits Schist, Connecticut, USA. Earth and Planetary Science Letters, 2020, 552, 116589.	1.8	28
54	Neoproterozoic extension and the Central Iapetus Magmatic Province in southern Mexico – New U-Pb ages, Hf-O isotopes and trace element data of zircon from the Chiapas Massif Complex. Gondwana Research, 2020, 88, 1-20.	3.0	15

#	Article	IF	CITATIONS
55	Causes and Consequences of Wehrlitization Beneath a Transâ€Lithospheric Fault: Evidence From Mesozoic Basaltâ€Borne Wehrlite Xenoliths From the Tanâ€Lu Fault Belt, North China Craton. Journal of Geophysical Research: Solid Earth, 2020, 125, e2019JB019084.	1.4	5
56	Metasomatic Evolution of Coesite-Bearing Diamondiferous Eclogite from the Udachnaya Kimberlite. Minerals (Basel, Switzerland), 2020, 10, 383.	0.8	14
57	Zircon U-Pb-Hf isotope systematics of Transvaal Supergroup – Constraints for the geodynamic evolution of the Kaapvaal Craton and its hinterland between 2.65 and 2.06ÂGa. Precambrian Research, 2020, 345, 105760.	1.2	26
58	Ultrapotassic magmatism in the heyday of the Variscan Orogeny: the story of the TÅ™ebÃÄ•Pluton, the largest durbachitic body in the Bohemian Massif. International Journal of Earth Sciences, 2020, 109, 1767-1810.	0.9	30
59	Nepheline syenite intrusions from the Rengali Province, eastern India: Integrating geological setting, microstructures, and geochronological observations on their syntectonic emplacement. Precambrian Research, 2020, 346, 105802.	1.2	2
60	Cadomian (ca. 550ÂMa) magmatic and thermal imprint on the North Arabian-Nubian Shield (south and) Tj ETQ	00 0 0 rgB 1,2 rgB	/Overlock 10
61	From hydroplastic to brittle deformation: Controls on fluid flow in fold and thrust belts. Insights from the Lower Pedraforca thrust sheet (SE Pyrenees). Marine and Petroleum Geology, 2020, 120, 104517.	1.5	16
62	Geochronological and geochemical data from fracture-filling calcites from the Lower Pedraforca thrust sheet (SE Pyrenees). Data in Brief, 2020, 31, 105896.	0.5	0
63	Tectonic Evolution of the Northern Oman Mountains, Part of the Strait of Hormuz Syntaxis: New Structural and Paleothermal Analyses and Uâ€Pb Dating of Synkinematic Calcite. Tectonics, 2020, 39, e2019TC005936.	1.3	18
64	Enigmatic 1146 ± 4ÂMa old granite in the southeastern rim of the West African craton, now part of the Dahomeyan orogenic belt in Ghana. Journal of African Earth Sciences, 2020, 167, 103814.	0.9	2
65	Hercynian anatexis in the envelope of the Beni Bousera peridotites (Alboran Domain, Morocco): Implications for the tectono-metamorphic evolution of the deep crustal roots of the Mediterranean region. Gondwana Research, 2020, 83, 157-182.	3.0	27
66	The missing link of Rodinia breakup in western South America: A petrographical, geochemical, and zircon Pb-Hf isotope study of the volcanosedimentary Chilla beds (Altiplano, Bolivia). , 2020, 16, 619-645.		11
67	Ultramafic Carbonated Melt―and Autoâ€Metasomatism in Mantle Eclogites: Compositional Effects and Geophysical Consequences. Geochemistry, Geophysics, Geosystems, 2020, 21, e2019GC008774.	1.0	24
68	Hafnium isotopic record of mantle-crust interaction in an evolving continental magmatic system. Earth and Planetary Science Letters, 2020, 535, 116100.	1.8	18
69	Characteristics and timing of hydrothermal fluid circulation in the fossil Pyrenean hyperextended rift system: new constraints from the Chaînons Béarnais (W Pyrenees). International Journal of Earth Sciences, 2020, 109, 1071-1093.	0.9	17
70	Mesozoic deposits of SW Gondwana (Namibia): unravelling Gondwanan sedimentary dispersion drivers by detrital zircon. International Journal of Earth Sciences, 2020, 109, 1683-1704.	0.9	10
71	Reconstruction of the prograde PT history of high―P migmatitic paragneisses via meltâ€reintegration approach and thermodynamic modelling (Allochthonous Complexes, NW Iberian Massif). Journal of Metamorphic Geology, 2020, 38, 629-653.	1.6	3
72	Updated geochronology and isotope geochemistry of the Vila de Cruces Ophiolite: a case study of a peri-Gondwanan back-arc ophiolite. Geological Society Special Publication, 2020, , SP503-2020-8.	0.8	8

IF # ARTICLE CITATIONS Diamondiferous and barren eclogites and pyroxenites from the western Kaapvaal craton record subduction processes and mantle metasomatism, respectively. Lithos, 2020, 368-369, 105588. Fault-controlled fluid circulation and diagenesis along basin-bounding fault systems in rifts – 74 1.2 6 insights from the East Greenland rift system. Solid Earth, 2020, 11, 1987-2013. Petrogenesis of fractionated nested granite intrusions: the SedmihoÅ™Ã-Composite Stock (Bohemian) Tj ETQq1 1 0.784314,rgBT /O HYDROTHERMAL MINERALISATION OF THE TATRIC SUPERUNIT (WESTERN CARPATHIANS, SLOVAKIA): II. GEOCHRONOLOGY AND TIMING OF MINERALISATIONS IN THE NAZKE TATRY MTS.. Geologica Carpathica, 76 0.2 1 2020, 71, . The geochronological history of the Hohnsdorf Crystalline Complex (Germany) $\hat{a} \in$ Piecing together the puzzling evolution of the Mid-German Crystalline Rise. Zeitschrift Der Deutschen Gesellschaft 0.1 Fur Geowissenschaften, 2020, 171, 121-133. Geochronological constraints on the carbonate-sulfarsenide veins in DobÅjinÃj, Slovakia: U/Pb ages of 78 hydrothermal carbonates, Re/Os age of gersdorffite, and K/Ar ages of fuchsite. Journal of Geosciences 0.3 2 (Czech Republic), 2020, , 229-247. Chronologic constraints on hominin dispersal outside Africa since 2.48â€⁻Ma from the Zarqa Valley, 79 1.4 Jordan. Quaternary Science Reviews, 2019, 219, 1-19. A unique recipe for glass beads at Iron Age Sardis. Journal of Archaeological Science, 2019, 108, 104974. 80 1.2 9 Longâ€Period Astronomical Forcing of Westerlies' Strength in Central Asia During Miocene Climate Cooling. Paleoceanography and Paleoclimatology, 2019, 34, 1784-1806. 1.3 Shallow reworking of magmatic zircon grains of latest Neoproterozoic (Timanian) age in serpentinite 82 of the Voykar Massif, Polar Urals: new constraints from U-Pb isotopic data, and first trace elements 0.4 1 and Lu-Hf isotopic data. Gff, 2019, 141, 253-262. Triassic evolution of the western Neotethys: constraints from microfabrics and U–Pb detrital zircon ages of the Plattenkalk Unit (External Hellenides, Greece). International Journal of Earth Sciences, 0.9 2019, 108, 2493-2529. Unusual marbles in a non-metamorphic succession of the SW Alps (Valdieri, Italy) due to early 84 0.9 5 Oligocene hydrothermal flow. International Journal of Earth Sciences, 2019, 108, 693-712. Effects of multi-stage rifting and metasomatism on HSE-187Os/188Os systematics of the cratonic 1.2 mantle beneath SW Greenland. Contributions To Mineralogy and Petrology, 2019, 174, 1. Two-pyroxene syenitoids from the Moldanubian Zone of the Bohemian Massif: Peculiar magmas derived 86 0.6 17 from a strongly enriched lithospheric mantle source. Lithos, 2019, 342-343, 239-262. The essence of time – fertile skarn formation in the Variscan Orogenic Belt. Earth and Planetary 1.8 Science Letters, 2019, 519, 165-170. Zircon Petrochronology and 40Ar/39Ar Thermochronology of the Adamello Intrusive Suite, N. Italy: Monitoring the Growth and Decay of an Incrementally Assembled Magmatic System. Journal of 88 1.1 38 Petrology, 2019, 60, 701-722. Correlation between Composition and Mechanical Properties of Calcium Silicate Hydrates Identified by Infrared Spectroscopy and Density Functional Theory. Journal of Physical Chemistry C, 2019, 123, 1.5 10868-10873. Dating of anatase-forming diagenetic reactions in Rotliegend sandstones of the North German Basin. 90 0.9 4 International Journal of Earth Sciences, 2019, 108, 1275-1292.

AXEL GERDES

#	Article	IF	CITATIONS
91	High-Mg and Low-Mg Mantle Eclogites from Koidu (West African Craton) Linked by Neoproterozoic Ultramafic Melt Metasomatism of Subducted Archaean Plateau-like Oceanic Crust. Journal of Petrology, 2019, 60, 723-754.	1.1	23
92	Development of an Intrawedge Tectonic Mélange by Outâ€of‣equence Thrusting, Buttressing, and Intraformational Rheological Contrast, Mt. Massico Ridge, Apennines, Italy. Tectonics, 2019, 38, 1223-1249.	1.3	25
93	U–Pb ages of magmatic and detrital zircon of the Döhlen Basin: geological history of a Permian strike-slip basin in the Elbe Zone (Germany). International Journal of Earth Sciences, 2019, 108, 887-910.	0.9	9
94	Archean Rare-Metal Pegmatites in Zimbabwe and Western Australia. SpringerBriefs in World Mineral Deposits, 2019, , .	0.5	15
95	Introduction to Archean Rare-Metal Pegmatites. SpringerBriefs in World Mineral Deposits, 2019, , 1-21.	0.5	2
96	Geological Settings of Archean Rare-Metal Pegmatites. SpringerBriefs in World Mineral Deposits, 2019, , 23-59.	0.5	1
97	Geochronology of Archean LCT Pegmatites. SpringerBriefs in World Mineral Deposits, 2019, , 87-94.	0.5	0
98	Genesis of Massive Pollucite Mineralisation in Archean LCT Pegmatites. SpringerBriefs in World Mineral Deposits, 2019, , 103-125.	0.5	0
99	Hafnium Isotopic Composition of the Bushveld Complex Requires Mantle Melt–Upper Crust Mixing: New Evidence from Zirconology of Mafic, Felsic and Metasedimentary Rocks. Journal of Petrology, 2019, 60, 2169-2200.	1.1	18
100	Element Transfer and Redox Conditions in Continental Subduction Zones: New Insights from Peridotites of the Ulten Zone, North Italy. Journal of Petrology, 2019, 60, 231-268.	1.1	13
101	Building up the first continents: Mesoarchean to Paleoproterozoic crustal evolution in West Troms, Norway, inferred from granitoid petrology, geochemistry and zircon U-Pb/Lu-Hf isotopes. Precambrian Research, 2019, 321, 303-327.	1.2	25
102	Multi-proxy isotopic tracing of magmatic sources and crustal recycling in the Palaeozoic to Early Jurassic active margin of North-Western Gondwana. Gondwana Research, 2019, 66, 227-245.	3.0	11
103	Provenance of exotic Ordovician and Devonian sedimentary rock units from the Rhenish Massif (Central European Variscides, Germany). Tectonophysics, 2019, 755, 127-159.	0.9	4
104	The nature and significance of the Faroe-Shetland Terrane: Linking Archaean basement blocks across the North Atlantic. Precambrian Research, 2019, 321, 154-171.	1.2	21
105	The Chemical Evolution from Older (323–318 Ma) towards Younger Highly Evolved Tin Granites (315–314 Ma)—Sources and Metal Enrichment in Variscan Granites of the Western Erzgebirge (Central) Tj E	:TQq.B10	.78 ≉ 314 rg81
106	The rise of feathered dinosaurs: <i>Kulindadromeus zabaikalicus</i> , the oldest dinosaur with †feather-like' structures. PeerJ, 2019, 7, e6239.	0.9	6
107	Formation conditions and REY enrichment of the 2060ÂMa phosphorus mineralization at Schiel (South) Tj ETQq	1 1 0.784 1.7	-314 rgBT /Cv
108	The First U–Pb Isotopic Systematics of Natural Aeschynite and Coexisting Monazite. Doklady Earth Sciences, 2018, 478, 82-87.	0.2	0

#	Article	IF	CITATIONS
109	A new U–Pb zircon age and a volcanogenic model for the early Permian Chemnitz Fossil Forest. International Journal of Earth Sciences, 2018, 107, 2465-2489.	0.9	18
110	Archean magmatic-hydrothermal fluid evolution in the Quadrilátero FerrÃfero (SE Brazil) documented by B isotopes (LA MC-ICPMS) in tourmaline. Chemical Geology, 2018, 481, 95-109.	1.4	25
111	The White Nile as a source for Nile sediments: Assessment using U-Pb geochronology of detrital rutile and monazite. Journal of African Earth Sciences, 2018, 140, 1-8.	0.9	7
112	Zircon (Hf, O isotopes) as melt indicator: Melt infiltration and abundant new zircon growth within melt rich layers of granulite-facies lenses versus solid-state recrystallization in hosting amphibolite-facies gneisses (central Erzgebirge, Bohemian Massif). Lithos, 2018, 302-303, 65-85.	0.6	14
113	New age constraints on the palaeoenvironmental evolution of the late Paleozoic back-arc basin along the western Gondwana margin of southern Peru. Journal of South American Earth Sciences, 2018, 82, 165-180.	0.6	6
114	Subduction factory in an ampoule: Experiments on sediment–peridotite interaction under temperature gradient conditions. Geochimica Et Cosmochimica Acta, 2018, 223, 319-349.	1.6	20
115	Reconstruction of a >200â€ [−] Ma multi-stage "five element―Bi-Co-Ni-Fe-As-S system in the Penninic Alps, Switzerland. Ore Geology Reviews, 2018, 95, 746-788.	1.1	27
116	Extensive reworking of Archaean crust within the Birimian terrane in Ghana as revealed by combined zircon U-Pb and Lu-Hf isotopes. Geoscience Frontiers, 2018, 9, 173-189.	4.3	35
117	Late Oligocene to early Miocene humidity change recorded in terrestrial sequences in the Ili Basin (southâ€eastern Kazakhstan, Central Asia). Sedimentology, 2018, 65, 517-539.	1.6	28
118	A new U–Pb LA-ICP-MS age of the Rumburk granite (Lausitz Block, Saxo-Thuringian Zone): constraints for a magmatic event in the Upper Cambrian. International Journal of Earth Sciences, 2018, 107, 933-953.	0.9	17
119	A ~565ÂMa old glaciation in the Ediacaran of peri-Gondwanan West Africa. International Journal of Earth Sciences, 2018, 107, 885-911.	0.9	55
120	The Diamantina Monazite: A New Lowâ€Th Reference Material for Microanalysis. Geostandards and Geoanalytical Research, 2018, 42, 25-47.	1.7	32
121	Late-stage anhydrite-gypsum-siderite-dolomite-calcite assemblages record the transition from a deep to a shallow hydrothermal system in the Schwarzwald mining district, SW Germany. Geochimica Et Cosmochimica Acta, 2018, 223, 259-278.	1.6	41
122	From Cadomian magmatic arc to Rheic ocean closure: The geochronological-geochemical record of nappe protoliths of the Münchberg Massif, NE Bavaria (Germany). Gondwana Research, 2018, 55, 135-152.	3.0	36
123	New U-Pb dates show a Paleogene origin for the modern Asian biodiversity hot spots. Geology, 2018, 46, 3-6.	2.0	74
124	Absolute ages of multiple generations of brittle structures by U-Pb dating of calcite. Geology, 2018, 46, 207-210.	2.0	121
125	U-Pb dating of calcite cement and diagenetic history in microporous carbonate reservoirs: Case of the Urgonian Limestone, France. Geology, 2018, 46, 247-250.	2.0	65
126	An emerging thermochronometer for carbonate-bearing rocks: â^†47 /(U-Pb). Geology, 2018, 46, 1067-1070.	2.0	60

#	Article	IF	CITATIONS
127	Anatectic Granitic Pegmatites from the Eastern Alps: A Case of Variable Rare-Metal Enrichment During High-Grade Regional Metamorphism – I: Mineral Assemblages, Geochemical Characteristics, and Emplacement Ages. Canadian Mineralogist, 2018, 56, 555-602.	0.3	27
128	First Results of U–Pb LA–ICP–MS Isotope Dating of Detrital Zircons from Arkose Sandstone of the Biryan Subformation of Zilmerdak Formation (Upper Riphean, South Urals). Doklady Earth Sciences, 2018, 482, 1275-1277.	0.2	20
129	New Detrital Zircon Geochronology From the Cycladic Basement (Greece): Implications for the Paleozoic Accretion of Periâ€Gondwanan Terranes to Laurussia. Tectonics, 2018, 37, 4679-4699.	1.3	25
130	Metamorphic P-T path and SIMS zircon U-Pb dating of amphibolite of the Namche Barwa Complex, southeast Tibet, China. Lithos, 2018, 320-321, 454-469.	0.6	12
131	Cambrian Magmatism in the Northern Urals: New Data on the Age and Formation Conditions. Doklady Earth Sciences, 2018, 481, 993-996.	0.2	0
132	Magmatic Mn-rich garnets in volcanic settings: Age and longevity of the magmatic plumbing system of the Miocene Ramadas volcanism (NW Argentina). Lithos, 2018, 322, 238-249.	0.6	19
133	Silica-rich septarian concretions in biogenic silica-poor sediments: A marker of hydrothermal activity at fossil hyper-extended rifted margins (Err nappe, Switzerland). Sedimentary Geology, 2018, 378, 19-33.	1.0	7
134	Neogene fluvial landscape evolution in the hyperarid core of the Atacama Desert. Scientific Reports, 2018, 8, 13952.	1.6	52
135	Provenance of the Surveyor Fan and Precursor Sediments in the Gulf of Alaska—Implications of a Combined U-Pb, (U-Th)/He, Hf, and Rare Earth Element Study of Detrital Zircons. Journal of Geology, 2018, 126, 577-600.	0.7	6
136	The lower crust of the Northern broken edge of Gondwana: Evidence for sediment subduction and syn-Variscan anorogenic imprint from zircon U-Pb-Hf in granulite xenoliths. Gondwana Research, 2018, 64, 84-96.	3.0	16
137	The Strandja Massif and the İstanbul Zone were once parts of the same palaeotectonic unit: new data from Triassic detrital zircons. Geodinamica Acta, 2018, 30, 212-224.	2.2	10
138	Combined zircon U Pb and Lu Hf isotopes study of magmatism and high-P metamorphism of the basal allochthonous units in the SW Iberian Massif (Ossa-Morena complex). Lithos, 2018, 322, 20-37.	0.6	23
139	In situ LA-ICPMS Isotopic and Geochronological Studies on Carbonatites and Phoscorites from the Guli Massif, Maymecha-Kotuy, Polar Siberia. Geochemistry International, 2018, 56, 766-783.	0.2	8
140	Reconstruction of late Holocene autumn/winter precipitation variability in SW Romania from a high-resolution speleothem trace element record. Earth and Planetary Science Letters, 2018, 499, 122-133.	1.8	41
141	Paleosols on the Ediacaran basalts of the East European Craton: A unique record of paleoweathering with minimum diagenetic overprint. Precambrian Research, 2018, 316, 66-82.	1.2	31
142	Age and temperature-time evolution of retrogressed eclogite-facies rocks in the Paleoproterozoic Nagssugtoqidian Orogen, South-East Greenland: Constrained from U-Pb dating of zircon, monazite, titanite and rutile. Precambrian Research, 2018, 314, 468-486.	1.2	24
143	Cadomian metasediments and Ordovician sandstone from Corsica: detrital zircon U–Pb–Hf constrains on their provenance and paleogeography. International Journal of Earth Sciences, 2018, 107, 2803-2818.	0.9	14
144	Synergies in elemental mobility during weathering of tetrahedrite [(Cu,Fe,Zn)12(Sb,As)4S13]: Field observations, electron microscopy, isotopes of Cu, C, O, radiometric dating, and water geochemistry. Chemical Geology, 2018, 488, 1-20.	1.4	18

#	Article	IF	CITATIONS
145	Sr, Nd, and Hf Isotope Composition of Rocks of the Reft Gabbro–Diorite–Tonalite Complex (Eastern) Tj ETQq2	1 1 0.7843 0.2	314 rgBT /〇 2
146	2018, 56, 495-508. The connection between hydrothermal fluids, mineralization, tectonics and magmatism in a continental rift setting: Fluorite Sm-Nd and hematite and carbonates U-Pb geochronology from the Rhinegraben in SW Germany. Geochimica Et Cosmochimica Acta, 2018, 240, 11-42.	1.6	47
147	Proterozoic to Cretaceous evolution of the western and central Pearya Terrane (Canadian High) Tj ETQq1 1 0.784	314 rgBT 0.7	/Qverlock 10
148	Thermal evolution in the exhumed basement of a stratovolcano: case study of the Miocene Mátra Volcano, Pannonian Basin. Journal of the Geological Society, 2018, 175, 820-835.	0.9	5
149	Mineralogical and chemical evolution of tantalum–(niobium–tin) mineralisation in pegmatites and granites. Part 2: Worldwide examples (excluding Africa) and an overview of global metallogenetic patterns. Ore Geology Reviews, 2017, 89, 946-987.	1.1	60
150	The Pelagonian terrane of Greece in the peri-Gondwanan mosaic of the Eastern Mediterranean: Implications for the geological evolution of Avalonia. Precambrian Research, 2017, 290, 163-183.	1.2	19
151	Magmatism and crustal extension: Constraining activation of the ductile shearing along the Gediz detachment, Menderes Massif (western Turkey). Lithos, 2017, 282-283, 145-162.	0.6	28
152	Tracing Proterozoic arc mantle Hf isotope depletion of southern Fennoscandia through coupled zircon U–Pb and Lu–Hf isotopes. Lithos, 2017, 284-285, 122-131.	0.6	6
153	In Situ Sr isotopes in Plagioclase and Trace Element Systematics in the Lowest Part of the Eastern Bushveld Complex: Dynamic Processes in an Evolving Magma Chamber. Journal of Petrology, 2017, 58, 327-360.	1.1	34
154	The Sr, Nd, and Hf isotopic geochemistry of rocks of the gabbro–diorite–tonalite association from the Eastern Segment of the Middle Urals as an indicator of the age of the continental crust in this area. Doklady Earth Sciences, 2017, 474, 516-519.	0.2	0
155	Petrogenesis of alkaline basalt-hosted sapphire megacrysts. Petrological and geochemical investigations of in situ sapphire occurrences from the Siebengebirge Volcanic Field, Germany. Contributions To Mineralogy and Petrology, 2017, 172, 1.	1.2	23
156	Assessing the isotopic evolution of S-type granites of the Carlos Chagas Batholith, SE Brazil: Clues from U–Pb, Hf isotopes, Ti geothermometry and trace element composition of zircon. Lithos, 2017, 284-285, 730-750.	0.6	33
157	The tectonometamorphic and magmatic evolution of the Uppermost Unit in central Crete (Melambes) Tj ETQq1 1 Research, 2017, 48, 50-71.	0.784314 3.0	4 rgBT /Over 10
158	Provenance of Upper Devonian clastic (meta)sediments of the Böllstein Odenwald (Mid-German-Crystalline-Zone, Variscides). International Journal of Earth Sciences, 2017, 106, 2927-2943.	0.9	13
159	A New Appraisal of Sri Lankan <scp>BB</scp> Zircon as a Reference MaterialÂfor LAâ€iCPâ€iMS Uâ€Pb Geochronology and Luâ€iff IsotopeÂTracing. Geostandards and Geoanalytical Research, 2017, 41, 335-358.	1.7	135
160	Fingerprinting fluid sources in Troodos ophiolite complex orbicular glasses using high spatial resolution isotope and trace element geochemistry. Geochimica Et Cosmochimica Acta, 2017, 200, 145-166.	1.6	20
161	Investigating the pore structure of the calcium silicate hydrate phase. Materials Characterization, 2017, 133, 133-137.	1.9	29
162	Source constraints on the genesis of Danubian granites in the South Carpathians Alpine Belt (Romania). Lithos, 2017, 294-295, 198-221.	0.6	3

#	Article	IF	CITATIONS
163	How do granitoid magmas mix with each other? Insights from textures, trace element and Sr–Nd isotopic composition of apatite and titanite from the Matok pluton (South Africa). Contributions To Mineralogy and Petrology, 2017, 172, 1.	1.2	62
164	Carbonate ooids of the Mesoarchaean Pongola Supergroup, South Africa. Geobiology, 2017, 15, 750-766.	1.1	28
165	Characterization of zircon reference materials via high precision U–Pb LA-MC-ICP-MS. Journal of Analytical Atomic Spectrometry, 2017, 32, 2011-2023.	1.6	49
166	First data on Early Carboniferous intrusive magmatism of the eastern margin of the Middle Urals: Geodynamic conditions and U–Pb isotope constraints. Doklady Earth Sciences, 2017, 476, 1038-1042.	0.2	0
167	New data concerning the age and specific features of magmatism of timanides in the southern part of the Lyapin structure (Northern Urals). Doklady Earth Sciences, 2017, 476, 1125-1129.	0.2	1
168	Detrital rutile U-Pb perspective on the origin of the great Cambro-Ordovician sandstone of North Gondwana and its linkage to orogeny. Gondwana Research, 2017, 51, 17-29.	3.0	48
169	The first Lu–Hf zircon isotope data for gabbro–diorite–tonalite associations of the Urals. Doklady Earth Sciences, 2017, 472, 104-108.	0.2	0
170	Geochemical and geochronological constraints on distinct Early-Neoproterozoic and Cambrian accretionary events along southern margin of the Baydrag Continent in western Mongolia. Gondwana Research, 2017, 47, 200-227.	3.0	57
171	Methane and the origin of five-element veins: Mineralogy, age, fluid inclusion chemistry and ore forming processes in the Odenwald, SW Germany. Ore Geology Reviews, 2017, 81, 42-61.	1.1	90
172	U-Pb geochronology on zircon and columbite-group minerals of the Cap de Creus pegmatites, NE Spain. Mineralogy and Petrology, 2017, 111, 1-21.	0.4	27
173	Origin of reverse compositional and textural zoning in granite plutons by localized thermal overturn of stratified magma chambers. Lithos, 2017, 277, 315-336.	0.6	7
174	Zircon Hafnium–Oxygen Isotope and Trace Element Petrochronology of Intraplate Volcanic Rocks from the Eifel (Germany) and Implications for Mantle versus Crustal Origins of Zircon Megacrysts. Journal of Petrology, 2017, 58, 1841-1870.	1.1	42
175	Volatile-rich Metasomatism in the Cratonic Mantle beneath SW Greenland: Link to Kimberlites and Mid-lithospheric Discontinuities. Journal of Petrology, 2017, 58, 2311-2338.	1.1	46
176	New data on the age and nature of the Khan–Bogd alkaline granites, Mongolia. Doklady Earth Sciences, 2017, 477, 1320-1324.	0.2	3
177	A Reconnaissance Study of Ti-minerals in Cratonic Granulite Xenoliths and their Potential as Recorders of Lower Crust Formation and Evolution. Journal of Petrology, 2017, 58, 2007-2034.	1.1	7
178	U–Pb and Lu–Hf Systematics of Zircons from Sargur Metasediments, Dharwar Craton, Southern India:New Insights on the Provenance and Crustal Evolution. Current Science, 2017, 113, 1394.	0.4	11
179	Seismic-stratigraphic architecture of the Oligocene-Pliocene CamanÃ _i Formation, southern Peruvian forearc (Province of Arequipa). Andean Geology, 2017, 44, 17.	0.2	4
180	The crustal evolution of South America from a zircon Hfâ€isotope perspective. Terra Nova, 2016, 28, 128-137.	0.9	28

#	Article	IF	CITATIONS
181	Rapid Middle Eocene temperature change in western North America. Earth and Planetary Science Letters, 2016, 450, 132-139.	1.8	50

182 New data on the composition and age of granitoids in the northern part of the Tagil structure (Ural) Tj ETQq0 0 0 rgBT /Overlock 10 Tf 5

183	The rim zone of cement-based materials – Barrier or fast lane for chemical degradation?. Cement and Concrete Composites, 2016, 74, 236-243.	4.6	4
184	U–Pb age of detrital zircon from the Embu sequence, Ribeira belt, Se Brazil. Precambrian Research, 2016, 278, 69-86.	1.2	31
185	U–Pb–Hf isotope systematics of detrital zircons in high-grade paragneisses of the Ancient Gneiss Complex, Swaziland: Evidence for two periods of juvenile crust formation, Paleo- and Mesoarchaean sediment deposition, and 3.23 Ga terrane accretion. Precambrian Research, 2016, 280, 205-220.	1.2	25
186	Characterisation of Triassic rifting in Peru and implications for the early disassembly of western Pangaea. Gondwana Research, 2016, 35, 124-143.	3.0	92
187	Formation of diamondiferous kyanite–eclogite in a subduction mélange. Geochimica Et Cosmochimica Acta, 2016, 179, 156-176.	1.6	29
188	Exotic crustal components at the northern margin of the Bohemian Massif—Implications from U Th Pb and Hf isotopes of zircon from the Saxonian Granulite Massif. Tectonophysics, 2016, 681, 234-249.	0.9	18
189	The ages and tectonic setting of the Faja Eruptiva de la Puna Oriental, Ordovician, NW Argentina. Lithos, 2016, 256-257, 41-54.	0.6	46
190	First U–Pb isotopic data on zircon from andesite of the Saf'yanovka Cu-bearing massive sulfide deposit (Middle Urals). Doklady Earth Sciences, 2016, 469, 665-669.	0.2	2
191	Separating regional metamorphic and metasomatic assemblages and events in the northern Khetri complex, NW India: Evidence from mineralogy, whole-rock geochemistry and U-Pb monazite chronology. Journal of Asian Earth Sciences, 2016, 129, 117-141.	1.0	30
192	Allochthonous terranes involved in the Variscan suture of NW Iberia: A review of their origin and tectonothermal evolution. Earth-Science Reviews, 2016, 161, 140-178.	4.0	71
193	Archean crustal evolution in the Southern São Francisco craton, Brazil: Constraints from U-Pb, Lu-Hf and O isotope analyses. Lithos, 2016, 266-267, 64-86.	0.6	56
194	Kinematics of the Alpenrhein-Bodensee graben system in the Central Alps: Oligocene/Miocene transtension due to formation of the Western Alps arc. Tectonics, 2016, 35, 1367-1391.	1.3	87
195	New structural and U–Pb zircon data from Anafi crystalline basement (Cyclades, Greece): constraints on the evolution of a Late Cretaceous magmatic arc in the Internal Hellenides. International Journal of Earth Sciences, 2016, 105, 2031-2060.	0.9	32
196	Crustal geodynamics from the Archaean Bundelkhand Craton, India: constraints from zircon U–Pb–Hf isotope studies. Geological Magazine, 2016, 153, 179-192.	0.9	81
197	History of the West African Neoproterozoic Ocean: Key to the geotectonic history of circum-Atlantic Peri-Gondwana (Adrar Souttouf Massif, Moroccan Sahara). Gondwana Research, 2016, 29, 220-233.	3.0	43
198	Early Variscan (Visean) granites in the core of central Pyrenean gneiss domes: implications from laser ablation U-Pb and Th-Pb studies. Gondwana Research, 2016, 29, 181-198.	3.0	44

#	Article	IF	CITATIONS
199	Tracking the late Paleozoic to early Mesozoic margin of northern Gondwana in the Hellenides: paleotectonic constraints from U–Pb detrital zircon ages. International Journal of Earth Sciences, 2016, 105, 1881-1899.	0.9	11
200	An assessment of monazite from the Itambé pegmatite district for use as U–Pb isotope reference material for microanalysis and implications for the origin of the "Moacyr―monazite. Chemical Geology, 2016, 424, 30-50.	1.4	94
201	Origin of the Eastern Mediterranean: Neotethys rifting along a cryptic Cadomian suture with Afro-Arabia. Bulletin of the Geological Society of America, 2016, 128, 1286-1296.	1.6	43
202	The calc-alkaline and adakitic volcanism of the Sabzevar structural zone (NE Iran): Implications for the Eocene magmatic flare-up in Central Iran. Lithos, 2016, 248-251, 517-535.	0.6	60
203	Implications of U–Pb and Lu–Hf isotopic analysis of detrital zircons for the depositional age, provenance and tectonic setting of the Permian–Triassic Palaeotethyan Karakaya Complex, NW Turkey. International Journal of Earth Sciences, 2016, 105, 7-38.	0.9	62
204	U–Pb and Hf isotope records in detrital and magmatic zircon from eastern and western Dharwar craton, southern India: Evidence for coeval Archaean crustal evolution. Precambrian Research, 2016, 275, 496-512.	1.2	58
205	Silurian U–Pb zircon age (LA-ICP-MS) of granitoids from the Zelenodol Cu–porphyry deposit, Southern Urals. Doklady Earth Sciences, 2016, 466, 92-95.	0.2	3
206	The last stages of the Avalonian–Cadomian arc in NW Iberian Massif: isotopic and igneous record for a long-lived peri-Gondwanan magmatic arc. Tectonophysics, 2016, 681, 6-14.	0.9	25
207	Strontium isotope systematics of scheelite and apatite from the Felbertal tungsten deposit, Austria – results of in-situ LA-MC-ICP-MS analysis. Mineralogy and Petrology, 2016, 110, 11-27.	0.4	32
208	Similar crustal evolution in the western units of the Adrar Souttouf Massif (Moroccan Sahara) and the Avalonian terranes: Insights from Hf isotope data. Tectonophysics, 2016, 681, 305-317.	0.9	19
209	U–Pb, Lu–Hf and trace element characteristics of zircon from the Felbertal scheelite deposit (Austria): New constraints on timing and source of W mineralization. Chemical Geology, 2016, 421, 112-126.	1.4	39
210	Mineralogy and mineral chemistry of detrital heavy minerals from the Rhine River in Germany as evidence to their provenance, sedimentary and depositional history: focus on platinum-group minerals and remarks on cassiterite, columbite-group minerals and uraninite. International Journal of Earth Sciences, 2016, 105, 637-657.	0.9	12
211	The Rudnik Mts. volcano-intrusive complex (central Serbia): An example of how magmatism controls metallogeny. Geologia Croatica, 2016, 69, 89-99.	0.3	7
212	Novel Thermo-Chronological Approaches of Carbonate Diagenesis Quantification (Δ47 and U/Pb): Case of the Paris Basin. , 2016, , .		0
213	First results of U–Pb dating of detrital zircons from metasandstones of the Isherim anticlinorium (North Urals). Doklady Earth Sciences, 2015, 464, 1010-1014.	0.2	12
214	Provenance of the <scp>HP</scp> – <scp>HT</scp> subducted margin in the Variscan belt (Cabo Ortegal) Tj E	TQq000	rgBT_/Overloc
215	U–Pb ages of apatite in the western Tauern Window (Eastern Alps): Tracing the onset of collision-related exhumation in the European plate. Earth and Planetary Science Letters, 2015, 418, 53-65	1.8	27

A Hf-isotope perspective on continent formation in the south Peruvian Andes. Geological Society 0.8 31 Special Publication, 2015, 389, 305-321.

#	Article	IF	CITATIONS
217	Closure of the Paleotethys in the External Hellenides: Constraints from U–Pb ages of magmatic and detrital zircons (Crete). Gondwana Research, 2015, 28, 642-667.	3.0	49
218	A hidden Tonian basement in the eastern Mediterranean: Age constraints from U–Pb data of magmatic and detrital zircons of the External Hellenides (Crete and Peloponnesus). Precambrian Research, 2015, 258, 83-108.	1.2	61
219	Validation of the determination of the B isotopic composition in Roman glasses with laser ablation multi-collector inductively coupled plasma-mass spectrometry. Spectrochimica Acta, Part B: Atomic Spectroscopy, 2015, 105, 116-120.	1.5	23
220	Carbonation of Wollastonite(001) Competing Hydration: Microscopic Insights from Ion Spectroscopy and Density Functional Theory. ACS Applied Materials & amp; Interfaces, 2015, 7, 4706-4712.	4.0	41
221	Mesoproterozoic continental growth: U–Pb–Hf–O zircon record in the Idefjorden Terrane, Sveconorwegian Orogen. Precambrian Research, 2015, 261, 75-95.	1.2	32
222	Reduced sediment melting at 7.5–12ÂGPa: phase relations, geochemical signals and diamond nucleation. Contributions To Mineralogy and Petrology, 2015, 170, 1.	1.2	34
223	Preservation of successive diagenetic stages in Middle Triassic bonebeds: Evidence from in situ trace element and strontium isotope analysis of vertebrate fossils. Chemical Geology, 2015, 410, 108-123.	1.4	16
224	A multiâ€system geochronology in the Adâ€3 borehole, Pannonian Basin (Hungary) with implications for dating volcanic rocks by lowâ€temperature thermochronology and for interpretation of (U–Th)/He data. Terra Nova, 2015, 27, 258-269.	0.9	23
225	REE and Lu-Hf systematics of zircons from rapakivi granites and associated rocks of supercontinent Nuna (Columbia). Doklady Earth Sciences, 2015, 461, 277-282.	0.2	2
226	Provenance of the Variscan Upper Allochthon (Cabo Ortegal Complex, NW Iberian Massif). Gondwana Research, 2015, 28, 1434-1448.	3.0	54
227	The detrital zircon U–Pb–Hf fingerprint of the northern Arabian–Nubian Shield as reflected by a Late Ediacaran arkosic wedge (Zenifim Formation; subsurface Israel). Precambrian Research, 2015, 266, 1-11.	1.2	51
228	Zircon U–Pb geochronology and heavy mineral composition of the Camaná Formation, southern Peru: Constraints on sediment provenance and uplift of the Coastal and Western Cordilleras. Journal of South American Earth Sciences, 2015, 61, 14-32.	0.6	7
229	The southern and central parts of the "Souttoufide―belt, Northwest Africa. Journal of African Earth Sciences, 2015, 112, 451-470.	0.9	27
230	Characterization of silane-based hydrophobic admixtures in concrete using TOF-MS. Cement and Concrete Research, 2015, 70, 77-82.	4.6	31
231	Cadomian basement and Paleozoic to Triassic siliciclastics of the Taurides (Karacahisar dome,) Tj ETQq1 1 0.784	314 rgBT / 0.6	Overlock 10
232	Linking the thermal evolution and emplacement history of an upper-crustal pluton to its lower-crustal roots using zircon geochronology and geochemistry (southern Adamello batholith, N.) Tj ETQqO 0 () r gB T /Ov	erl sz k 10 Tf 5
233	Role of crustal contribution in the early stage of the Damara Orogen, Namibia: New constraints from combined U–Pb and Lu–Hf isotopes from the Goas Magmatic Complex. Gondwana Research, 2015, 28, 961-986.	3.0	37

234Immediate impact on the rim zone of cement based materials due to chemical attack. Materials
Characterization, 2015, 99, 77-83.1.97

#	Article	IF	CITATIONS
235	Tantalum–(niobium–tin) mineralisation in African pegmatites and rare metal granites: Constraints from Ta–Nb oxide mineralogy, geochemistry and U–Pb geochronology. Ore Geology Reviews, 2015, 64, 667-719.	1.1	187
236	Arc-related Ediacaran magmatism along the northern margin of Gondwana: Geochronology and isotopic geochemistry from northern Iberia. Gondwana Research, 2015, 27, 216-227.	3.0	44
237	The four Neoproterozoic glaciations of southern Namibia and their detrital zircon record: The fingerprints of four crustal growth events during two supercontinent cycles. Precambrian Research, 2015, 259, 176-188.	1.2	45
238	In situ U–Pb isotopic dating of columbite–tantalite by LA–ICP–MS. Ore Geology Reviews, 2015, 65, 979-989.	1.1	110
239	Tectonic setting and geochronology of the Cadomian (Ediacaran-Cambrian) magmatism in Central Iran, Kuh-e-Sarhangi region (NW Lut Block). Journal of Asian Earth Sciences, 2015, 102, 24-44.	1.0	74
240	Origin and provenance of igneous clasts from late Palaeozoic conglomerate formations (Del Ratón) Tj ETQq0 0 C 2014, 40, .) rgBT /Ov 0.6	erlock 10 Tf 5
241	New data on the composition and age of complexes in the pre-Paleozoic basement of the Tagil Paleo-island arc system in the Northern Urals. Doklady Earth Sciences, 2014, 459, 1499-1503.	0.2	4
242	The Alapaevsk-Sukhoi Log porphyry copper zone, Middle Urals: The U-Pb age of productive magmatism. Doklady Earth Sciences, 2014, 459, 1479-1482.	0.2	3
243	New data on composition and age of granites from the Isherim anticlinorium and boundary of the Timanides in the North Urals. Doklady Earth Sciences, 2014, 459, 1514-1518.	0.2	6
244	Detrital zircon U–Pb–Hf systematics of Israeli coastal sands: new perspectives on the provenance of Nile sediments. Journal of the Geological Society, 2014, 171, 107-116.	0.9	30
245	Two-stage collision: Exploring the birth of Pangea in the Variscan terranes. Gondwana Research, 2014, 25, 756-763.	3.0	97
246	The East Variscan Shear Zone: Geochronological constraints from the Capo Ferro area (NE Sardinia,) Tj ETQq0 0 0	rgBT /Ove	erlock 10 Tf !
247	Re-interpreting the Devonian ophiolites involved in the Variscan suture: U–Pb and Lu–Hf zircon data of the Moeche Ophiolite (Cabo Ortegal Complex, NW Iberia). International Journal of Earth Sciences, 2014, 103, 1385-1402.	0.9	49
248	Crustal evolution of the Southern Granulite Terrane, south India: New geochronological and geochemical data for felsic orthogneisses and granites. Precambrian Research, 2014, 246, 91-122.	1.2	133
249	Peri-Amazonian provenance of the Proto-Pelagonian basement (Greece), from zircon U–Pb geochronology and Lu–Hf isotopic geochemistry. Lithos, 2014, 184-187, 379-392.	0.6	40
250	Constraining genesis and geotectonic setting of metavolcanic complexes: a multidisciplinary study of the Devonian Vrbno Group (Hrubý JesenÃk Mts., Czech Republic). International Journal of Earth Sciences, 2014, 103, 455-483.	0.9	36
251	Mantle eclogites and garnet pyroxenites – the meaning of two-point isochrons, Sm–Nd and Lu–Hf closure temperatures and the cooling of the subcratonic mantle. Earth and Planetary Science Letters, 2014, 389, 143-154.	1.8	39
252	The oldest zircons of Africa—Their U–Pb–Hf–O isotope and trace element systematics, and implications for Hadean to Archean crust–mantle evolution. Precambrian Research, 2014, 241, 203-230.	1.2	83

#	Article	IF	CITATIONS
253	Permo-Triassic anatexis, continental rifting and the disassembly of western Pangaea. Lithos, 2014, 190-191, 383-402.	0.6	98
254	Adakite differentiation and emplacement in a subduction channel: The late Paleocene Sabzevar magmatism (NE Iran). Bulletin of the Geological Society of America, 2014, 126, 317-343.	1.6	63
255	Small-scale Hf isotopic variability in the Peninsula pluton (South Africa): the processes that control inheritance of source 176Hf/177Hf diversity in S-type granites. Contributions To Mineralogy and Petrology, 2014, 168, 1.	1.2	75
256	Petrography, geochemistry and U–Pb zircon age of the Matongo carbonatite Massif (Burundi): Implication for the Neoproterozoic geodynamic evolution of Central Africa. Journal of African Earth Sciences, 2014, 100, 656-674.	0.9	21
257	The Namuskluft and Dreigratberg sections in southern Namibia (Kalahari Craton, Gariep Belt): a geological history of Neoproterozoic rifting and recycling of cratonic crust during the dispersal of Rodinia until the amalgamation of Gondwana. International Journal of Earth Sciences, 2014, 103, 1187-1202.	0.9	38
258	Krasnotur'insk Skarn copper ore field, Northern Urals: The U-Pb age of ore-controlling diorites and their place in the regional metallogeny. Doklady Earth Sciences, 2014, 456, 641-645.	0.2	7
259	HFSE (High Field Strength Elements)-transport and U–Pb–Hf isotope homogenization mediated by Ca-bearing aqueous fluids at 2.04Ga: Constraints from zircon, monazite, and garnet of the Venetia Klippe, Limpopo Belt, South Africa. Geochimica Et Cosmochimica Acta, 2014, 138, 81-100.	1.6	38
260	The Cadomian Orogen: Neoproterozoic to Early Cambrian crustal growth and orogenic zoning along the periphery of the West African Craton—Constraints from U–Pb zircon ages and Hf isotopes (Schwarzburg Antiform, Germany). Precambrian Research, 2014, 244, 236-278.	1.2	245
261	The intubation scoop (iâ€scoop) – a new type of laryngoscope for difficult and normal airways. Anaesthesia, 2014, 69, 990-1001.	1.8	4
262	Ages of protolith and Neoproterozoic metamorphism of Al-P-bearing quartzites of the Veredas formation (Northern Espinhaço, Brazil): LA-ICP-MS age determinations on relict and recrystallized zircon and geodynamic consequences. Precambrian Research, 2014, 250, 6-26.	1.2	13
263	Distinguishing between in-situ and accretionary growth of continents along active margins. Lithos, 2014, 202-203, 382-394.	0.6	64
264	Carbonated sediment–peridotite interaction and melting at 7.5–12GPa. Lithos, 2014, 200-201, 368-385.	0.6	36
265	The Saxothuringian-Rhenohercynian boundary underneath the Vogelsberg volcanic field: evidence from basement xenoliths and U-Pb zircon data of trachyte. Zeitschrift Der Deutschen Gesellschaft Fur Geowissenschaften, 2014, 165, 373-394.	0.1	4
266	Provenance Analysis of the Late Ediacaran Basins from Southwestern Iberia (Série Negra Succession) Tj ETQq0) 0 0 rgBT	/Overlock 10
267	The Cadomian Orogen: Neoproterozoic to Early Cambrian Crustal Growth and Orogenic Zoning Along the Northwestern Periphery of the West African Craton. Springer Geology, 2014, , 729-732.	0.2	2
268	Crustal Evolution of the Northeast Laurentian Margin and the Peri-Gondwanan Microcontinent Ganderia Prior to and During Closure of the Iapetus Ocean: Detrital Zircon U–Pb and Hf Isotope Evidence from Newfoundland. Geoscience Canada, 2014, 41, 345.	0.3	40
269	Provenance of Cambrian–Ordovician Siliciclastic Rocks of Southwestern Iberia: Insights into the Evolution of the North Gondwana Margin. Springer Geology, 2014, , 753-757.	0.2	0
270	Tracking the evolution of large-volume silicic magma reservoirs from assembly to supereruption. Geology, 2013, 41, 867-870.	2.0	226

#	Article	IF	CITATIONS
271	Uâ€Pb Detrital Zircon Analysis – Results of an Interâ€laboratory Comparison. Geostandards and Geoanalytical Research, 2013, 37, 243-259.	1.7	95
272	New data on the composition and age of orogenic granitoids from Timanides of the North Urals. Doklady Earth Sciences, 2013, 450, 618-622.	0.2	5
273	Nature of magmatism and sedimentation at a Columbia active margin: Insights from combined U–Pb and Lu–Hf isotope data of detrital zircons from NW India. Gondwana Research, 2013, 23, 1040-1052.	3.0	100
274	Crustal source of the Late Cretaceous Satansarı monzonite stock (central Anatolia – Turkey) and its significance for the Alpine geodynamic evolution. Journal of Geodynamics, 2013, 65, 82-93.	0.7	26
275	The oldest magmatic formation of the uralides in the north Urals. Doklady Earth Sciences, 2013, 453, 1185-1187.	0.2	1
276	The lithospheric mantle underneath the Gibeon Kimberlite field (Namibia): A mix of old and young components—Evidence from Lu–Hf and Sm–Nd isotope systematics. Precambrian Research, 2013, 231, 263-276.	1.2	9
277	The effect of amphibolite facies metamorphism on the U–Th–Pb geochronology of accessory minerals from meta-carbonatites and associated meta-alkaline rocks. Chemical Geology, 2013, 353, 199-209.	1.4	25
278	Constraints on Variscan and Cimmerian magmatism and metamorphism in the Pontides (Yusufeli–Artvin area), NE Turkey from U–Pb dating and granite geochemistry. Geological Society Special Publication, 2013, 372, 49-74.	0.8	58
279	Geochronological and geochemical constraints on the formation and evolution of the mantle underneath the Kaapvaal craton: Lu–Hf and Sm–Nd systematics of subcalcic garnets from highly depleted peridotites. Geochimica Et Cosmochimica Acta, 2013, 113, 1-20.	1.6	35
280	Sveconorwegian Mid-crustal Ultrahigh-temperature Metamorphism in Rogaland, Norway: U-Pb LA-ICP-MS Geochronology and Pseudosections of Sapphirine Granulites and Associated Paragneisses. Journal of Petrology, 2013, 54, 305-350. Instrume http://www.w3.org/1998/Math/MathML	1.1	49
281	altimg= si1.gif_overflow= scroll > <mml:mi>i </mml:mi> <mml:mmultiscripts><mml:mrow><mml:mrow><mml:mrow><mml:mrow><mml:mrow><mml:mrow><mml:mrow><mml:mrow><mml:mrow><mml:mrow><mml:mrow><mml:mrow><mml:mrow><mml:mrow><mml:mrow><mml:mrow><mml:mrow><mml:mrow><mml:mrow><mml:mrow><mml:mrow><mml:mrow><mml:mrow><mml:mrow><mml:mrow><mml:mrow><mml:mrow><mml:mrow><mml:mrow><mml:mrow><mml:mrow><mml:mrow><mml:mrow><mml:mrow><mml:mrow><mml:mrow><mml:mrow><mml:mrow><mml:mrow><mml:mrow><mml:mrow><mml:mrow><mml:mrow><mml:mrow><mml:mrow><mml:mrow><mml:mrow><mml:mrow><mml:mrow><mml:mrow><mml:mrow><mml:mrow><mml:mrow><mml:mrow><mml:mrow><mml:mrow><mml:mrow><mml:mrow><mml:mrow><mml:mrow><mml:mrow><mml:mrow><mml:mrow><mml:mrow><mml:mrow><mml:mrow><mml:mrow><mml:mrow><mml:mrow><mml:mrow><mml:mrow><mml:mrow><mml:mrow><mml:mrow><mml:mrow><mml:mrow><mml:mrow><mml:mrow><mml:mrow><mml:mrow><mml:mrow><mml:mrow><mml:mrow><mml:mrow><mml:mrow><mml:mrow><mml:mrow><mml:mrow><mml:mrow><mml:mrow><mml:mrow><mml:mrow><mml:mrow><mml:mrow><mml:mrow><mml:mrow><mml:mrow><mml:mrow><mml:mrow><mml:mrow><mml:mrow><mml:mrow><mml:mrow><mml:mrow><mml:mrow><mml:mrow><mml:mrow><mml:mrow><mml:mrow><mml:mrow><mml:mrow><mml:mrow><mml:mrow><mml:mrow><mml:mrow><mml:mrow><mml:mrow><mml:mrow><mml:mrow><mml:mrow><mml:mrow><mml:mrow><mml:mrow><mml:mrow><mml:mrow><mml:mrow><mml:mrow><mml:mrow><mml:mrow><mml:mrow><mml:mrow><mml:mrow><mml:mrow><mml:mrow><mml:mrow><mml:mrow><mml:mrow><mml:mrow><mml:mrow><mml:mrow><mml:mrow><mml:mrow><mml:mrow><mml:mrow><mml:mrow><mml:mrow><mml:mrow><mml:mrow><mml:mrow><mml:mrow><mml:mrow><mml:mrow><mml:mrow><mml:mrow><mml:mrow><mml:mrow><mml:mrow><mml:mrow><mml:mrow><mml:mrow><mml:mrow><mml:mrow><mml:mrow><mml:mrow><mml:mrow><mml:mrow><mml:mrow><mml:mrow><mml:mrow><mml:mrow><mml:mrow><mml:mrow><mml:mrow><mml:mrow><mml:mrow><mml:mrow><mml:mrow><mml:mrow><mml:mrow><mml:mrow><mml:mrow><mml:mrow><mml:mrow><mml:mrow><mml:mrow><mml:mrow><mml:mrow><mml:mrow><mml:mrow><mml:mrow><mml:mrow><mml:mrow><mml:mrow><mml:mrow><mml:mrow><mml:mrow><mml:mrow><mml< td=""><td>/><mml:no 1.8</mml:no </td><td>ne 40</td></mml<></mml:mrow></mml:mrow></mml:mrow></mml:mrow></mml:mrow></mml:mrow></mml:mrow></mml:mrow></mml:mrow></mml:mrow></mml:mrow></mml:mrow></mml:mrow></mml:mrow></mml:mrow></mml:mrow></mml:mrow></mml:mrow></mml:mrow></mml:mrow></mml:mrow></mml:mrow></mml:mrow></mml:mrow></mml:mrow></mml:mrow></mml:mrow></mml:mrow></mml:mrow></mml:mrow></mml:mrow></mml:mrow></mml:mrow></mml:mrow></mml:mrow></mml:mrow></mml:mrow></mml:mrow></mml:mrow></mml:mrow></mml:mrow></mml:mrow></mml:mrow></mml:mrow></mml:mrow></mml:mrow></mml:mrow></mml:mrow></mml:mrow></mml:mrow></mml:mrow></mml:mrow></mml:mrow></mml:mrow></mml:mrow></mml:mrow></mml:mrow></mml:mrow></mml:mrow></mml:mrow></mml:mrow></mml:mrow></mml:mrow></mml:mrow></mml:mrow></mml:mrow></mml:mrow></mml:mrow></mml:mrow></mml:mrow></mml:mrow></mml:mrow></mml:mrow></mml:mrow></mml:mrow></mml:mrow></mml:mrow></mml:mrow></mml:mrow></mml:mrow></mml:mrow></mml:mrow></mml:mrow></mml:mrow></mml:mrow></mml:mrow></mml:mrow></mml:mrow></mml:mrow></mml:mrow></mml:mrow></mml:mrow></mml:mrow></mml:mrow></mml:mrow></mml:mrow></mml:mrow></mml:mrow></mml:mrow></mml:mrow></mml:mrow></mml:mrow></mml:mrow></mml:mrow></mml:mrow></mml:mrow></mml:mrow></mml:mrow></mml:mrow></mml:mrow></mml:mrow></mml:mrow></mml:mrow></mml:mrow></mml:mrow></mml:mrow></mml:mrow></mml:mrow></mml:mrow></mml:mrow></mml:mrow></mml:mrow></mml:mrow></mml:mrow></mml:mrow></mml:mrow></mml:mrow></mml:mrow></mml:mrow></mml:mrow></mml:mrow></mml:mrow></mml:mrow></mml:mrow></mml:mrow></mml:mrow></mml:mrow></mml:mrow></mml:mrow></mml:mrow></mml:mrow></mml:mrow></mml:mrow></mml:mrow></mml:mrow></mml:mrow></mml:mrow></mml:mrow></mml:mrow></mml:mrow></mml:mrow></mml:mrow></mml:mrow></mml:mrow></mml:mrow></mml:mrow></mml:mrow></mml:mrow></mml:mrow></mml:mrow></mml:mrow></mml:mrow></mml:mrow></mml:mrow></mml:mrow></mml:mrow></mml:mrow></mml:mrow></mml:mrow></mml:mrow></mml:mrow></mml:mrow></mml:mrow></mml:mrow></mml:mrow></mml:mrow></mml:mrow></mml:mrow></mml:mrow></mml:mrow></mml:mrow></mml:mrow></mml:mrow></mml:mrow></mml:mrow></mml:mrow></mml:mrow></mml:mrow></mml:mrow></mml:mrow></mml:mrow></mml:mrow></mml:mrow></mml:mrow></mml:mrow></mml:mrow></mml:mrow></mml:mmultiscripts>	/> <mml:no 1.8</mml:no 	ne 40
282	Evolution and provenance of Neoproterozoic basement and Lower Paleozoic siliciclastic cover of the Menderes Massif (western Taurides): Coupled U–Pb–Hf zircon isotope geochemistry. Gondwana Research, 2013, 23, 682-700.	3.0	77
283	Timing of incremental pluton construction and magmatic activity in a back-arc setting revealed by ID-TIMS U/Pb and Hf isotopes on complex zircon grains. Chemical Geology, 2013, 342, 76-93.	1.4	54
284	Trace element partitioning between mantle minerals and silico-carbonate melts at 6–12GPa and applications to mantle metasomatism and kimberlite genesis. Lithos, 2013, 160-161, 183-200.	0.6	72
285	Different zircon recrystallization types in carbonatites caused by magma mixing: Evidence from U–Pb dating, trace element and isotope composition (Hf and O) of zircons from two Precambrian carbonatites from Fennoscandia. Chemical Geology, 2013, 353, 173-198.	1.4	43
286	Neoproterozoic to early Cambrian Franciscan-type mélanges in the TeplÃj–Barrandian unit, Bohemian Massif: Evidence of modern-style accretionary processes along the Cadomian active margin of Gondwana?. Precambrian Research, 2013, 224, 653-670.	1.2	43
287	U–Pb and Hf isotope data of detrital zircons from the Barberton Greenstone Belt: constraints on provenance and Archaean crustal evolution. Journal of the Geological Society, 2013, 170, 215-223.	0.9	70
288	Origin and evolution of Avalonia: evidence from U–Pb and Lu–Hf isotopes in zircon from the Mira terrane, Canada, and the Stavelot–Venn Massif, Belgium. Journal of the Geological Society, 2013, 170, 769-784.	0.9	73

#	Article	IF	CITATIONS
289	Reconstruction of the early Mesozoic plate margin of Gondwana by U–Pb ages of detrital zircons from northern Victoria Land, Antarctica. Geological Society Special Publication, 2013, 383, 211-232.	0.8	16
290	3.8 Ga zircons sampled by Neogene ignimbrite eruptions in Central Anatolia: COMMENT. Geology, 2013, 41, e307-e307.	2.0	3
291	The eclogite facies gneisses of the Cabo Ortegal Complex (NW Iberian Massif): Tectonothermal evolution and exhumation model. Journal of Iberian Geology, 2013, 38, .	0.7	5
292	Marins Granite (MG/SP): petrography, geochemistry, geochronology, and geotectonic setting. Brazilian Journal of Geology, 2013, 43, 487-500.	0.3	14
293	Evolution of the Early Permian volcanic-plutonic complex in the western part of the Permian Gobi-Altay Rift (Khar Argalant Mts., SW Mongolia). Journal of Geosciences (Czech Republic), 2012, , 105-126.	0.3	4
294	Geochemical and structural constraints on the magmatic history of the Chandman Massif of the eastern Mongolian Altay Range, SW Mongolia. Journal of Geosciences (Czech Republic), 2012, , 335-352.	0.3	2
295	An Early Ordovician tonalitic–granodioritic belt along the Schistose-Greywacke Domain of the Central Iberian Zone (Iberian Massif, Variscan Belt). Geological Magazine, 2012, 149, 927-939.	0.9	50
296	U–Pb detrital zircon analysis of the lower allochthon of NW Iberia: age constraints, provenance and links with the Variscan mobile belt and Gondwanan cratons. Journal of the Geological Society, 2012, 169, 655-665.	0.9	52
297	Petrology and age of metamorphosed rock in tectonic slices inside the Palaeozoic sediments of the eastern Mongolian Altay, SW Mongolia. Journal of Geosciences (Czech Republic), 2012, , 139-165.	0.3	13
298	Burd Gol Granite Massif as a product of the Late Cambrian post-orogenic magmatism in the SE part of the Lake Zone, Gobi Altay, SW Mongolia. Journal of Geosciences (Czech Republic), 2012, , 369-386.	0.3	4
299	U-Pb zircon constraints on the age of the Cretaceous Mata Amarilla Formation, Southern Patagonia, Argentina: its relationship with the evolution of the Austral Basin. Andean Geology, 2012, 39, .	0.2	49
300	Resolving the Variscan evolution of the Moldanubian sector of the Bohemian Massif: the significance of the Bavarian and the Moravo-Moldanubian tectonometamorphic phases. Journal of Geosciences (Czech Republic), 2012, , 9-28.	0.3	58
301	U–Pb and Hf isotope record of detrital zircons from gold-bearing sediments of the Pietersburg Greenstone Belt (South Africa)—Is there a common provenance with the Witwatersrand Basin?. Precambrian Research, 2012, 204-205, 46-56.	1.2	104
302	1000–580Ma crustal evolution in the northern Arabian-Nubian Shield revealed by U–Pb–Hf of detrital zircons from late Neoproterozoic sediments (Elat area, Israel). Precambrian Research, 2012, 208-211, 197-212.	1.2	76
303	Insights on the crustal evolution of the West African Craton from Hf isotopes in detrital zircons from the Anti-Atlas belt. Precambrian Research, 2012, 212-213, 263-274.	1.2	62
304	U-Pb Ages of Detrital Zircons from the Permo-Triassic Series of the Iberian Ranges: A Record of Variable Provenance during Rift Propagation. Journal of Geology, 2012, 120, 135-154.	0.7	17
305	New data on the composition and hafnium isotopes of zircons from carbonatites of the Khibiny Massif. Doklady Earth Sciences, 2012, 446, 1083-1085.	0.2	5
306	North-Gondwana assembly, break-up and paleogeography: U–Pb isotope evidence from detrital and igneous zircons of Ediacaran and Cambrian rocks of SW Iberia. Gondwana Research, 2012, 22, 866-881.	3.0	115

#	Article	IF	CITATIONS
307	U–Th–Pb geochronology of meta-carbonatites and meta-alkaline rocks in the southern Canadian Cordillera: A geodynamic perspective. Lithos, 2012, 152, 202-217.	0.6	55
308	Bunker Cave stalagmites: an archive for central European Holocene climate variability. Climate of the Past, 2012, 8, 1751-1764.	1.3	81
309	Crustal homogenization revealed by U–Pb zircon ages and Hf isotope evidence from the Late Cretaceous granitoids of the Agaçören intrusive suite (Central Anatolia/Turkey). Contributions To Mineralogy and Petrology, 2012, 163, 725-743.	1.2	29
310	The Bazar Ophiolite of NW Iberia: a relic of the Iapetus–Tornquist Ocean in the Variscan suture. Terra Nova, 2012, 24, 283-294.	0.9	40
311	Coupled U–Pb–Hf of detrital zircons of Cambrian sandstones from Morocco and Sardinia: Implications for provenance and Precambrian crustal evolution of North Africa. Gondwana Research, 2012, 21, 690-703.	3.0	159
312	Evidence of Precambrian sedimentation/magmatism and Cambrian metamorphism in the Bitlis Massif, SE Turkey utilising whole-rock geochemistry and U–Pb LA-ICP-MS zircon dating. Gondwana Research, 2012, 21, 1001-1018.	3.0	82
313	U–Pb, trace element and Lu–Hf properties of unique dissolution–reprecipitation zircon from UHP eclogite in SW Sulu terrane, eastern China. Gondwana Research, 2012, 22, 169-183.	3.0	29
314	Monazite stability, composition and geochronology as tracers of Paleoproterozoic events at the eastern margin of the East European Craton (Taratash complex, Middle Urals). Lithos, 2012, 132-133, 82-97.	0.6	15
315	Late Neoproterozoic P-T evolution of HP-UHT Granulites from the Palni Hills (South India): New Constraints from Phase Diagram Modelling, LA-ICP-MS Zircon Dating and in-situ EMP Monazite Dating. Journal of Petrology, 2011, 52, 1813-1856.	1.1	86
316	Longâ€lived orogenic construction along the paleoâ€Pacific margin of Gondwana (Deep Freeze Range,) Tj ETQq(0 0 0 rgBT 1.3	/Overlock 10
317	Dating of Pleistocene uranyl phosphates in the supergene alteration zone of Late Variscan granites by Laser-Ablation-Inductive-Coupled-Plasma Mass Spectrometry with a review of U minerals of geochronological relevance to Quaternary geology. Chemie Der Erde, 2011, 71, 201-206.	0.8	5
318	Hafnium isotope record of the Ancient Gneiss Complex, Swaziland, southern Africa: evidence for Archaean crust–mantle formation and crust reworking between 3.66 and 2.73 Ga. Journal of the Geological Society, 2011, 168, 953-964.	0.9	139
319	Isotope geochemistry and revised geochronology of the Purrido Ophiolite (Cabo Ortegal Complex,) Tj ETQq1 1 0 Journal of the Geological Society, 2011, 168, 733-750.	0.784314 r 0.9	gBT /Overloc 43
320	Crustal evolution and recycling in the northern Arabian-Nubian Shield: New perspectives from zircon Lu–Hf and U–Pb systematics. Precambrian Research, 2011, 186, 101-116.	1.2	160
321	Archaean to Palaeoproterozoic crustal evolution of the Aravalli mountain range, NW India, and its hinterland: The U–Pb and Hf isotope record of detrital zircon. Precambrian Research, 2011, 187, 155-164.	1.2	107
322	The AmmarnäComplex in the central Scandinavian Caledonides: an allochthonous basin fragment in the foreland of the Sveconorwegian orogen?. Terra Nova, 2011, 23, 270-279.	0.9	6
323	Speeding Up the Analytical Workflow for Coltan Fingerprinting by an Integrated Mineral Liberation Analysis/LAâ€ICPâ€MS Approach. Geostandards and Geoanalytical Research, 2011, 35, 431-448.	1.7	44
324	Provenance of Neoproterozoic and early Paleozoic siliciclastic rocks of the TeplÃi-Barrandian unit (Bohemian Massif): Evidence from U–Pb detrital zircon ages. Gondwana Research, 2011, 19, 213-231.	3.0	145

#	Article	IF	CITATIONS
325	Detrital zircon ages from a Lower Ordovician quartzite of the İstanbul exotic terrane (NW Turkey): evidence for Amazonian affinity. International Journal of Earth Sciences, 2011, 100, 23-41.	0.9	72
326	Multiple accretion at the eastern margin of the Rio de la Plata craton: the prolonged Brasiliano orogeny in southernmost Brazil. International Journal of Earth Sciences, 2011, 100, 355-378.	0.9	107
327	The geodynamics of collision of a microplate (Chilenia) in Devonian times deduced by the pressure–temperature–time evolution within part of a collisional belt (Guarguaraz Complex,) Tj ETQq1 1 0.7	84824 rgE	BT \$ @verlock.
328	Late Neoproterozoic overprinting of the cassiterite and columbite-tantalite bearing pegmatites of the Gatumba area, Rwanda (Central Africa). Journal of African Earth Sciences, 2011, 61, 10-26.	0.9	90
329	New age data from the Dzirula massif, Georgia: Implications for the evolution of the Caucasian Variscides. Numerische Mathematik, 2011, 311, 404-441.	0.7	39
330	Detrital zircon Hf isotopic composition indicates long-distance transport of North Gondwana Cambrian–Ordovician sandstones. Geology, 2011, 39, 955-958.	2.0	84
331	The MoslavaÄka Gora crystalline massif in Croatia: a Cretaceous heat dome within remnant Ordovician granitoid crust. Swiss Journal of Geosciences, 2010, 103, 61-82.	0.5	12
332	Zircon U–Pb ages, REE concentrations and Hf isotope compositions of granitic leucosome and pegmatite from the north Sulu UHP terrane in China: Constraints on the timing and nature of partial melting. Lithos, 2010, 117, 247-268.	0.6	113
333	Baltica- and Gondwana-derived sediments in the Mid-German Crystalline Rise (Central Europe): Implications for the closure of the Rheic ocean. Gondwana Research, 2010, 17, 254-263.	3.0	101
334	U–Pb ages of detrital zircons from the Basal allochthonous units of NW Iberia: Provenance and paleoposition on the northern margin of Gondwana during the Neoproterozoic and Paleozoic. Gondwana Research, 2010, 18, 385-399.	3.0	149
335	Geodynamic evolution of the early Paleozoic Western Gondwana margin 14°–17°S reflected by the detritus of the Devonian and Ordovician basins of southern Peru and northern Bolivia. Gondwana Research, 2010, 18, 370-384.	3.0	69
336	Protective or damage promoting effect of calcium carbonate layers on the surface of cement based materials in aqueous environments. Cement and Concrete Research, 2010, 40, 1410-1418.	4.6	28
337	Early Cretaceous migmatitic mafic granulites from the Sabzevar range (NE Iran): implications for the closure of the Mesozoic peri-Tethyan oceans in central Iran. Terra Nova, 2010, 22, 26-34.	0.9	97
338	The behavior of the Hf isotope system in radiation-damaged zircon during experimental hydrothermal alteration. American Mineralogist, 2010, 95, 1343-1348.	0.9	80
339	Decompressional Heating of the Mahalapye Complex (Limpopo Belt, Botswana): a Response to Palaeoproterozoic Magmatic Underplating?. Journal of Petrology, 2010, 51, 703-729.	1.1	46
340	Magmatism and early-Variscan continental subduction in the northern Gondwana margin recorded in zircons from the basal units of Galicia, NW Spain. Bulletin of the Geological Society of America, 2010, 122, 219-235.	1.6	110
341	CLAY MINERALOGY AND LA-ICP-MS DATING OF SUPERGENE U-Cu NONTRONITE-BEARING MINERALIZATION AT NABBURG-WOLSENDORF, SOUTHEASTERN GERMANY. Canadian Mineralogist, 2010, 48, 497-511.	0.3	11
342	The multistage exhumation history of the Kaghan Valley UHP series, NW Himalaya, Pakistan from U-Pb and 40Ar/39Ar ages. European Journal of Mineralogy, 2010, 22, 703-719.	0.4	81

#	Article	IF	CITATIONS
343	Multi-method chronometric constraints on the evolution of the Northern Kyrgyz Tien Shan granitoids (Central Asian Orogenic Belt): From emplacement to exhumation. Journal of Asian Earth Sciences, 2010, 38, 131-146.	1.0	207
344	Hafnium isotope homogenization during metamorphic zircon growth in amphibolite-facies rocks: Examples from the Shackleton Range (Antarctica). Geochimica Et Cosmochimica Acta, 2010, 74, 4740-4758.	1.6	76
345	Age and mineralogy of supergene uranium minerals — Tools to unravel geomorphological and palaeohydrological processes in granitic terrains (Bohemian Massif, SE Germany). Geomorphology, 2010, 117, 44-65.	1.1	47
346	Constraining the physical–chemical conditions of Pleistocene cavernous weathering in Late Paleozoic granites. Geomorphology, 2010, 121, 283-290.	1.1	11
347	U–Th–Pb and Lu–Hf systematics of zircon from TTG's, leucosomes, meta-anorthosites and quartzites of the Limpopo Belt (South Africa): Constraints for the formation, recycling and metamorphism of Palaeoarchaean crust. Precambrian Research, 2010, 179, 50-68.	1.2	153
348	Detrital zircon ages of Neoproterozoic sequences of the Moroccan Anti-Atlas belt. Precambrian Research, 2010, 181, 115-128.	1.2	141
349	Reworking of Earth's first crust: Constraints from Hf isotopes in Archean zircons from Mt. Narryer, Australia. Precambrian Research, 2010, 182, 175-186.	1.2	73
350	New constraints on the auriferous Witwatersrand sediment provenance from combined detrital zircon U–Pb and Lu–Hf isotope data for the Eldorado Reef (Central Rand Group, South Africa). Precambrian Research, 2010, 183, 817-824.	1.2	41
351	Zirconium and hafnium in meteorites. Meteoritics and Planetary Science, 2010, 45, 1136-1151.	0.7	13
352	Unique coesite-bearing zircon from allanite-bearing gneisses: U-Pb, REE and Lu-Hf properties and implications for the evolution of the Sulu UHP terrane, China. European Journal of Mineralogy, 2010, 21, 1225-1250.	0.4	25
353	Timing and modes of granite magmatism in the core of the Alboran Domain, Rif chain, northern Morocco: Implications for the Alpine evolution of the western Mediterranean. Tectonics, 2010, 29, n/a-n/a.	1.3	59
354	In situ LA-SF-ICP-MS U-Pb dating of metasomatic zircon growth during retrogression of UHP eclogites, Sulu deep drilling hole, China. European Journal of Mineralogy, 2010, 21, 1251-1264.	0.4	9
355	Timing of dextral strike-slip processes and basement exhumation in the Elbe Zone (Saxo-Thuringian) Tj ETQq1 1 0. zircon data. Geological Society Special Publication, 2009, 327, 197-214.	784314 rg 0.8	gBT /Overl <mark>oc</mark> 24
356	HERCYNIAN AGE OF THE COBALT-NICKEL-ARSENIDE-(GOLD) ORES, BOU AZZER, ANTI-ATLAS, MOROCCO: Re-Os, Sm-Nd, AND U-Pb AGE DETERMINATIONS. Economic Geology, 2009, 104, 1065-1079.	1.8	41
357	Origin of fayalite granitoids: New insights from the Cobquecura Pluton, Chile, and its metapelitic xenoliths. Lithos, 2009, 110, 181-198.	0.6	24
358	Differential subduction and exhumation of crustal slices in the Sulu HPâ€UHP metamorphic terrane: insights from mineral inclusions, trace elements, Uâ€Pb and Luâ€Hf isotope analyses of zircon in orthogneiss. Journal of Metamorphic Geology, 2009, 27, 805-825.	1.6	65
359	Zircon formation versus zircon alteration — New insights from combined U–Pb and Lu–Hf in-situ LA-ICP-MS analyses, and consequences for the interpretation of Archean zircon from the Central Zone of the Limpopo Belt. Chemical Geology, 2009, 261, 230-243.	1.4	639
360	Precise and accurate in situ U–Pb dating of zircon with high sample throughput by automated LA-SF-ICP-MS. Chemical Geology, 2009, 261, 261-270.	1.4	381

#	Article	IF	CITATIONS
361	Palaeoproterozoic to Palaeozoic magmatic and metamorphic events in the Shackleton Range, East Antarctica: Constraints from zircon and monazite dating, and implications for the amalgamation of Gondwana. Precambrian Research, 2009, 172, 25-45.	1.2	52
362	Archean Accretion and Crustal Evolution of the Kalahari Craton—the Zircon Age and Hf Isotope Record of Granitic Rocks from Barberton/Swaziland to the Francistown Arc. Journal of Petrology, 2009, 50, 933-966.	1.1	290
363	Unraveling Sedimentary Provenance and Tectonothermal History of Highâ€Temperature Metapelites, Using Zircon and Monazite Chemistry: A Case Study from the Eastern Ghats Belt, India. Journal of Geology, 2009, 117, 665-683.	0.7	82
364	Measuring 0.01‰ to 0.1‰ isotopic variations by MC-ICPMS—testing limits for the first time with Pb Î-iCRMs. Journal of Analytical Atomic Spectrometry, 2009, 24, 407.	1.6	11
365	HERCYNIAN AGE OF THE COBALT-NICKEL-ARSENIDE-(GOLD) ORES, BOU AZZER, ANTI-ATLAS, MOROCCO: Re-Os, Sm-Nd, AND U-Pb AGE DETERMINATIONS. Economic Geology, 2009, 104, 1065-1079.	1.8	6
366	The Saxo-Danubian Granite Belt: magmatic response to post-collisional delamination of mantle lithosphere below the southwestern sector of the Bohemian Massif (Variscan orogen). Geologica Carpathica, 2009, 60, 205-212.	0.2	74
367	Miocene emplacement and rapid cooling of the Pohorje pluton at the Alpine-Pannonian-Dinaridic junction, Slovenia. Swiss Journal of Geosciences, 2008, 101, 255-271.	0.5	58
368	U-Pb zircon ages and geochemical data for the Monumental Granite and other granitoid rocks from Aswan, Egypt: implications for the geological evolution of the western margin of the Arabian Nubian Shield. Mineralogy and Petrology, 2008, 93, 153-183.	0.4	35
369	THE ORIGIN AND ZONING OF HYPOGENE AND SUPERGENE Fe-Mn-Mg-Sc-U-REE PHOSPHATE MINERALIZATION FROM THE NEWLY DISCOVERED TRUTZHOFMUHLE APLITE, HAGENDORF PEGMATITE PROVINCE, GERMANY. Canadian Mineralogist, 2008, 46, 1131-1157.	0.3	31
370	Neoarchaean high-grade metamorphism in the Central Zone of the Limpopo Belt (South Africa): Combined petrological and geochronological evidence from the Bulai pluton. Lithos, 2008, 103, 333-351.	0.6	63
371	The Cadomian Orogeny and the opening of the Rheic Ocean: The diacrony of geotectonic processes constrained by LA-ICP-MS U–Pb zircon dating (Ossa-Morena and Saxo-Thuringian Zones, Iberian and) Tj ETQq1	1 0.9 843	143 rg8 T /Ove
372	Natural fractionation of 238U/235U. Geochimica Et Cosmochimica Acta, 2008, 72, 345-359.	1.6	409
373	SHRIMP U–Pb dating, trace elements and the Lu–Hf isotope system of coesite-bearing zircon from amphibolite in the SW Sulu UHP terrane, eastern China. Geochimica Et Cosmochimica Acta, 2008, 72, 2973-3000.	1.6	150
374	U–Pb and Lu–Hf isotope record of detrital zircon grains from the Limpopo Belt – Evidence for crustal recycling at the Hadean to early-Archean transition. Geochimica Et Cosmochimica Acta, 2008, 72, 5304-5329.	1.6	95
375	PleÅjovice zircon — A new natural reference material for U–Pb and Hf isotopic microanalysis. Chemical Geology, 2008, 249, 1-35.	1.4	3,858
376	History of crustal growth and recycling at the Pacific convergent margin of South America at latitudes 29°–36° S revealed by a U–Pb and Lu–Hf isotope study of detrital zircon from late Paleozoic accretionary systems. Chemical Geology, 2008, 253, 114-129.	1.4	117
377	Post-Variscan to Early Alpine sedimentary basins in the Tauern Window (eastern Alps). Geological Society Special Publication, 2008, 298, 83-100.	0.8	10
378	Palaeoarchaean (3.3 Ga) mafic magmatism and Palaeoproterozoic (2.02 Ga) amphibolite-facies metamorphism in the Central Zone of the Limpopo Belt: New geochronological, petrological and geochemical constraints from metabasic and metapelitic rocks from the Venetia area. South African Journal of Geology, 2008, 111, 387-408.	0.6	24

#	Article	IF	CITATIONS
379	Geological setting of the Guelb Moghrein Fe oxide-Cu-Au-Co mineralization, Akjoujt area, Mauritania. Geological Society Special Publication, 2008, 297, 53-75.	0.8	10
380	Reply to Discussion by Romer (2008) <i>Mineralogical Magazine</i> , 72, 827–831. Mineralogical Magazine, 2008, 72, 833-835.	0.6	0
381	The Fe-Mn phosphate aplite â€~Silbergrube' near Waidhaus, Germany: epithermal phosphate mineralization in the Hagendorf-Pleystein pegmatite province. Mineralogical Magazine, 2008, 72, 1119-1144.	0.6	9
382	Miocene emplacement and rapid cooling of the Pohorije pluton at the Alpine-Pannonian-Dinaridic junction, Slovenia. Swiss Journal of Geosciences Supplement, 2008, , S255-S271.	0.0	2
383	Cu-Fe-U phosphate mineralization of the Hagendorf-Pleystein pegmatite province, Germany: with special reference to laser-ablation inductively-coupled plasma mass spectrometry (LA-ICP-MS) of limonite-cored torbernite. Mineralogical Magazine, 2007, 71, 371-387.	0.6	39
384	The continuum between Cadomian orogenesis and opening of the Rheic Ocean: Constraints from LA-ICP-MS U-Pb zircon dating and analysis of plate-tectonic setting (Saxo-Thuringian zone,) Tj ETQq0 0 0 rgBT /Ov	erlock 10	T 160 537 To
385	Zoned Zircon from Eclogite Lenses in Marbles from the Dabieâ€6ulu UHP Terrane, China: A Clear Record of Ultraâ€deep Subduction and Fast Exhumation. Acta Geologica Sinica, 2007, 81, 204-225.	0.8	28
386	Archaean to Proterozoic Crustal Evolution in the Central Zone of the Limpopo Belt (South) Tj ETQq0 0 0 rgBT /Ove Petrology, 2007, 48, 1605-1639.	erlock 10 ⁻ 1.1	Tf 50 467 Td 265
387	Clasts of Variscan highâ€grade rocks within Upper Viséan conglomerates – constraints on exhumation history from petrology and Uâ€Pb chronology. Journal of Metamorphic Geology, 2007, 25, 781-801.	1.6	43
388	Combined U–Pb and Hf isotope LA-(MC-)ICP-MS analyses of detrital zircons: Comparison with SHRIMP and new constraints for the provenance and age of an Armorican metasediment in Central Germany. Earth and Planetary Science Letters, 2006, 249, 47-61.	1.8	711
389	DETERMINATION OF 238U/235U, 236U/238U AND URANIUM CONCENTRATION IN URINE USING SF-ICP-MS AND MC-ICP-MS: AN INTERLABORATORY COMPARISON. Health Physics, 2006, 90, 127-138.	0.3	41
390	SHRIMP Uâ€Pb zircon dating from Suluâ€Dabie dolomitic marble, eastern China: constraints on prograde, ultrahighâ€pressure and retrograde metamorphic ages. Journal of Metamorphic Geology, 2006, 24, 569-589.	1.6	197
391	New ages from the Mauritanides Belt: recognition of Archean IOCG mineralization at Guelb Moghrein, Mauritania. Terra Nova, 2006, 18, 345-352.	0.9	31
392	Low-pressure Granulites of the Lišov Massif, Southern Bohemia: Viséan Metamorphism of Late Devonian Plutonic Arc Rocks. Journal of Petrology, 2006, 47, 705-744.	1.1	98
393	Provenance and Magmatic–Metamorphic Evolution of a Variscan Island-Arc Complex: Constraints from U–Pb Dating, Petrology, and Geospeedometry of the KyffhĀ ¤ ser Crystalline Complex, Central Germany. Journal of Petrology, 2005, 46, 1393-1420.	1.1	15
394	The Problem of Dating High-pressure Metamorphism: a U-Pb Isotope and Geochemical Study on Eclogites and Related Rocks of the Marianske Lazne Complex, Czech Republic. Journal of Petrology, 2004, 45, 1311-1338.	1.1	106
395	Magma-mixing in the genesis of Hercynian calc-alkaline granitoids: an integrated petrographic and geochemical study of the Sázava intrusion, Central Bohemian Pluton, Czech Republic. Lithos, 2004, 78, 67-99.	0.6	224
396	Chitinozoa and Nd isotope stratigraphy of the Ordovician rocks in the Ebbe Anticline, NW Germany. Geological Society Special Publication, 2002, 201, 115-131.	0.8	6

#	Article	IF	CITATIONS
397	Insights into the architecture and evolution of the Southern and Middle Urals from gravity and magnetic data. Geophysical Monograph Series, 2002, , 49-65.	0.1	9
398	Four decades of geochronological work in the Southern and Middle Urals: A review. Geophysical Monograph Series, 2002, , 233-255.	0.1	16
399	Palaeozoic amalgamation of Central Europe: new results from recent geological and geophysical investigations. Tectonophysics, 2002, 360, 5-21.	0.9	186
400	The syn- and post-orogenic low temperature events in the Southern and Middle Urals: Evidence from fission-track analysis. Geophysical Monograph Series, 2002, , 257-272.	0.1	8
401	Peraluminous granites frequently with mantle-like isotope compositions: the continental-type Murzinka and Dzhabyk batholiths of the eastern Urals. International Journal of Earth Sciences, 2002, 91, 3-19.	0.9	78
402	Magma homogenization during anatexis, ascent and/or emplacement? Constraints from the Variscan Weinsberg Granites. Terra Nova, 2001, 13, 305-312.	0.9	28
403	Hybrids, magma mixing and enriched mantle melts in post-collisional Variscan granitoids: the Rastenberg Pluton, Austria. Geological Society Special Publication, 2000, 179, 415-431.	0.8	33
404	Single-zircon evaporation ages and Rb–Sr dating of four major Variscan batholiths of the Urals. Tectonophysics, 2000, 317, 93-108.	0.9	58
405	Postâ€collisional granite generation and HT–LP metamorphism by radiogenic heating: the Variscan South Bohemian Batholith. Journal of the Geological Society, 2000, 157, 577-587.	0.9	154
406	Cadomian tectonics. , 0, , 103-154.		21
407	Advanced in situ geochronological and trace element microanalysis by laser ablation techniques. Geological Survey of Denmark and Greenland Bulletin, 0, 10, 25-28.	2.0	21
408	Dating blueschist-facies metamorphism within the Naga ophiolite, Northeast India, using sheared carbonate veins. International Geology Review, 0, , 1-18.	1.1	2